

Particle morphology and transport phenomena in olefin polymerisation

Christine Martin, Timothy F. McKenna*

LCCP-CNRS/ESCPE-Lyon, 43 Blvd du 11 Novembre 1918, 69616 Villeurbanne Cedex, France

Received 18 April 2001; accepted 2 August 2001

Abstract

Inverse gas chromatography has been used to estimate the characteristic mass transfer time for diffusion of ethylene and propylene in polypropylene particles. It was found that the mass transfer time corresponded to a length scale that is the same order of magnitude as the particle diameter, d_p (between 0.3 and 1 μm). Furthermore, when interpreted in terms of diffusion coefficients for spherical particles, these coefficients were found to be of the same order of magnitude and those measured elsewhere for diffusion in pure polymer. This implies that diffusion in the particles is controlled by diffusion in the polymer, and that previous descriptions of particle morphology used in modelling studies need to be revised. In addition, experimental evaluation of reaction rates has demonstrated that changing length scales due to particle agglomeration can also significantly reduce the observed activity in gas phase olefin polymerisation, and that the severity of the reduction in rate correlates with the severity of the agglomeration process. © 2002 Elsevier Science B.V. All rights reserved.

Keywords: Olefin polymerisation; Heat transfer; Mass transfer; Melt down; Morphology

1. Introduction

An important route for the production of polyolefins is the polymerisation of ethylene, propylene and/or α -olefin co-monomers, in gas or liquid phase processes using supported catalysts. At the risk of over-simplifying, the one thing that all of the different catalysts (Ziegler–Natta, metallocene, or chromium-based systems) have in common is that the active sites are deposited on and inside porous solid supports. In order to polymerise, the monomer must diffuse from the bulk phase to the active sites. During the very first instants of the reaction, this means that it is transported through the pores of the catalyst support. However, once the initial layer of polymer is formed on top of the active sites, the monomer must also dissolve in and diffuse through the polymer layer before it can react. As the reaction progresses, the polymer layer becomes thicker and thicker, and the original solid support fragments. Nevertheless, the particle retains its component parts because the polymer holds them together.

The exact shape of the particle fragments of the original structure (suspended in a continuous polymer matrix) will be determined by a number of factors, notably the mechanical strength and chemical nature of the support, the rate of reaction and the phase(s) present in the reactor.

However, as we stated above, monomer must diffuse from the bulk phase of the reactor, through the polymer covering the active sites, then to the sites located at the surface of the fragments. The concentration of monomer at the active sites will determine the rate of reaction (productivity) and composition of the polymer (product quality and molecular weight).

Before we consider the measurement of diffusion times, let us very briefly review the models currently used to model mass transfer in growing polyolefin particles. The most widely used models are the Multigrain Model (MGM), and its simpler analogue, the Polymeric Flow Model (PFM), both of which are shown schematically in Fig. 1.

In the MGM, one considers the growing particle (macrograin) to be an assembly of concentric layers of spherical fragments (micrograins). The model for mass transfer with chemical reaction is divided into two levels: the macrograin, with mass balance model being written

$$\frac{\partial C_{1,i}}{\partial t} = \frac{1}{r^2} \frac{\partial}{\partial r} \left(r^2 D_{\text{eff}} \frac{\partial C_{1,i}}{\partial r} \right) - R_{pi} \quad (1)$$

$$C_{1,i} = C_{1,i}^0, \quad \text{at } t = 0 \quad (1a)$$

$$\frac{\partial C_{1,i}}{\partial r} = 0, \quad \text{at } r = 0 \quad (1b)$$

$$C_{1,i} = C_{1,i}^{\text{bulk}}, \quad \text{at } r = r_p \quad (1c)$$

* Corresponding author. Tel.: +33-4-72-43-17-75.

E-mail address: mckenna@cpe.fr (T.F. McKenna).

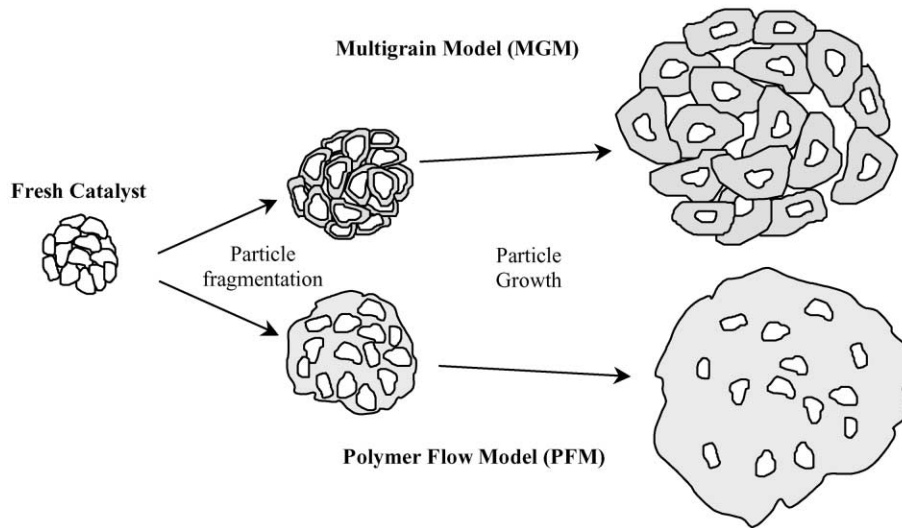


Fig. 1. Schematic representation of MGM and PFM descriptions of particle morphology.

and the micrograin

$$\frac{\partial C_{2,i}}{\partial t} = \frac{1}{r_2^2} \frac{\partial}{\partial r_2} \left(r_2^2 D_{pi} \frac{\partial C_{2,i}}{\partial r_2} \right) \quad (2)$$

$$C_{2,i} = C_{2,i}^{\text{eq}}, \quad \text{at } r_2 = r_{\text{mg}} \quad (2a)$$

$$C_{2,i} = C_{2,i}^0, \quad \text{at } t = 0 \quad (2b)$$

$$D_{pi} \frac{\partial C_{2,i}}{\partial r} = k_{pi} C^* C_{2,i}, \quad \text{at } r_2 = r_c \quad (2c)$$

In these expressions, r are r_2 are the radial co-ordinates of the macro- and micrograins, respectively, $C_{1,i}$ and $C_{2,i}$ the concentration of monomer in the same, D_{eff} and D_{pi} the diffusivity of monomer in the macroparticle and in the polyolefin phase, respectively, r_p and r_{mg} the radius of the macro- and micrograins respectively, r_c the radius of the micrograin crystals, $C_{2,i}^{\text{eq}}$ the concentration of monomer in the polymer in equilibrium with $C_{1,i}(r)$. Finally, R_{pi} is the volumetric rate of consumption of 'i' in the macroparticle, and is the term that links the macro- and microparticle balances. The boundary condition in (2c) comes from the equality of the diffusive flux and the rate of polymerisation at the active sites. C^* is the concentration of active sites on the surface of the micrograins. However, as we will be focusing on characteristic times for mass transfer and particle morphology, and not modelling diffusion inside the polymer particles, we will not discuss the strengths or weaknesses of Eq. (2) further. For more on this, see [1–3].

The polymeric flow model is a simplified version of the MGM, where we consider that the mass transfer resistance at the level of the micrograins is negligible. This means that we do not need to solve the set of Eq. (2), and the concentration of monomer at the active sites at any given spot in the particle is said to be in equilibrium with the concentration of monomer in the pores of the particle, found

by solving Eq. (1). As suggested in Fig. 1, the polymer flow model treats the particle as a pseudo-homogeneous medium with an effective diffusion coefficient that corresponds to the diffusion in the pores of the polymer matrix.

In either case, the models either implicitly or explicitly assume the existence of micrograins, suppose that the critical length scale for diffusion in the particles is the radius of the macrograin, and that the length scale for diffusion through the polymer phase is at most the thickness of the layer of polymer surrounding the micrograins. These last two points are important, especially in situations where difficulties with heat transfer can increase the thickness of this layer. Consider the definition of the characteristic mass transfer time

$$t_d = \frac{L^2}{D_{\text{eff}}}$$

where L is the characteristic length scale for mass transfer (e.g. particle radius for pseudo-homogeneous diffusion in the macroparticle, or polymer layer thickness in a microparticle) and D_{eff} is the effective diffusivity. In a gas phase polymerisation, the value of D_{eff} in the pores of the macroparticle has been estimated in the range of 10^{-4} to 10^{-3} cm^2/s , whereas in the polymer layer, it is on the order of 10^{-8} to 10^{-6} cm^2/s . This means that there is approximately four orders of magnitude difference between the two. Thus, diffusion in the polymer layer will be faster than that in the macroparticle as long as the difference in the effective diffusivity coefficients is on this order of magnitude, and as long as the characteristic length scale for diffusion in the polymer layer above the active sites remains two orders of magnitude (or more) smaller than that for the macroparticle. If either the effective diffusion coefficient in the macroparticle decreases and/or the length scale for diffusion in the polymer change so that these conditions are not true, diffusion through the polymer will become the dominant means of mass transfer

in the particles. This could have a significantly impact on mass transfer, polymerisation rates and polymer properties.

An interesting, inexpensive technique for the estimation of both monomer solubility and characteristic mass transfer time in non-reacting polyolefin particles was presented in an earlier study [4]. The derivation of the models for the interpretation of data is proposed in [4,5], so it will not be presented here. Let us simply recall that the method is based on the measurement of the dispersion of a peak of monomer injected on a chromatographic column filled with polyolefin powders.

2. Experimental

A scheme of the IGC technique and the diffusivities involved is shown in Fig. 2. The interested reader is referred to [4,5] for details on the experimental set-up. Different columns were packed with polymer in the form of particles as they are obtained in the reactor, and thus with morphology and microstructure similar to those one would find in real situations. A series of experiments was carried out using different polymer samples as column filling (only polypropylene and impact co-polymers will be considered here), and with ethylene and propylene as diffusing species. The powders were sieved and the different particle cuts listed in Table 1 were used to fill the columns. The column is heated to 80 °C, the injector to 100 °C, and the detector to 150 °C. The gas is injected into the injector with a gas syringe of 1 ml and the flow rate of the vector gas (helium) is comprised between 5 and 60 cm³/min.

Table 1
Properties of PP powders used in IGC experiments

Polypropylene	Density (g/cm ³)	Crystallinity (mass %) ^a	Void fraction by Hg porosimetry
DSM iPP	0.89	47 (25)	0.04
		46 (80)	
Solvay PP1	0.90	52 (25)	0.05
		51 (80)	
Solvay PP2	0.90	52 (25)	0.15
		52 (80)	
ATO PP1 × PP2	0.90	50 (25)	0.02
		50 (80)	

^a Values in parentheses are expressed in °C.

Gas phase polymerisation were carried out in a 2l, stainless steel semi-batch reactor. Three Zeigler–Natta catalysts (TiCl₄ on MgCl₂) were used in this work. Two of these products are commercial products donated to our laboratories and for reasons of industrial propriety, we cannot discuss the recipes for their production. The third catalyst, VM, was produced in our laboratories as described in [6,7]. All were used in exactly the same way. Monomers (ethylene and butene) were purchased from Air Liquide (France) and were of laboratory quality (>99.9% purity). They were used as received.

Before beginning the reaction, a small amount of inert high density polyethylene (HDPE) powder (about 15 g), which is used to disperse the catalyst, was stirred under vacuum in the reactor at 80 °C for 30 min. Monomer was fed from a ballast containing ethylene and from 0 to 4% butene (to help accelerate the polymerisation kinetics)

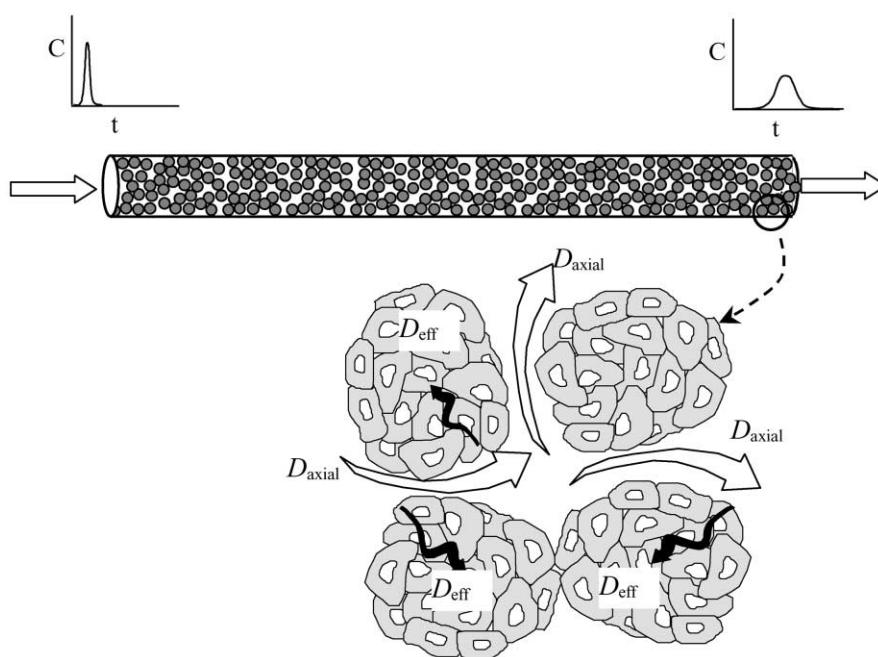


Fig. 2. Schematic diagram of inverse gas chromatographic experiment, and different mechanisms of diffusion in the column: D_{eff} characterises the diffusion in the porous particles, and D_{axial} represents the axial diffusion in the chromatographic column.

equipped with a pressure sensor. The catalyst powder (about 10 mg) was dispersed on 1–2 g or more of the same HDPE in a small glass balloon under inert atmosphere. Three millilitres of a solution of 1 M TEA in heptane was then injected onto the catalyst. The resulting mixing was finally dried under vacuum and agitation in order to eliminate the solvent. The catalyst powder was added to the reactor (corresponds to time, $t = 0$) with pressure of ethylene slightly above atmospheric pressure and at low stirring rate (~ 50 rpm). This was done 15 min after the first contact between catalyst and TEA. About 200 cm^3 (STP) of H_2 was then added in one shot. An additional amount of butene (0.5–1 bar) is also added during the reaction through a separate valve in order to maintain the equilibrium concentration imposed by the reactivity difference of the two monomers. The stirring rate was increased to approximately 250 rpm. The reactor temperature and the monomer pressure in the reactor were then increased to desired levels over the course of 4–5 min (desired levels 8 bar, 80°C). The reaction was then allowed to progress to the desired extent. Kinetics are evaluated by following the pressure drop in the ballast tank as a function of time (see [5,15] for details).

3. Results and discussion

3.1. Mass transfer

Solubility data, as well as information on the characteristic monomer mass transfer times in the particles of which the column is composed can be readily extracted from IGC experiments. Correctly choosing the experimental operating conditions (i.e. flow rates, column lengths, and measurement of dead volumes, etc.) allows one to use the theory of moments to interpret the chromatographic peaks obtained after injecting different gases on polymeric columns. The data obtained from these inverse chromatographic experiments allows one to directly calculate K , the ratio of concentration of penetrant in the column support at equilibrium to concentration of penetrant in carrier gas, and a characteristic mass transfer time, t_m , defined as follows:

$$t_m = t_a + t_e + t_d \quad (3)$$

where t_a is the time constant of absorption on the surface of the solid support (i.e. polymer particles), t_e the characteristic time for mass transfer through the particle boundary layer, and t_d the characteristic diffusion time. If one correctly chooses the flow rate (see [4,5]) then t_a and t_e can reasonably be supposed to be negligible, in which case the dominant means of mass transfer in the (porous) solid phase of the chromatographic column (i.e. the particles) will be the diffusion of the penetrant. This means that expression (3) can be simplified to $t_m = t_d$, where the characteristic diffusion time is proportional to the length

Table 2

The t_m data for C_2H_4 on different polyolefin powders [5]

Polymer (d_p) (μm)	t_m (s)
ATO PP1 (215)	3.4
ATO PP2 (462.5)	14.3
Solvay PP1 (362.5)	9.1
Solvay PP2 (362.5)	1.9

squared divided by the effective diffusion coefficient in the particles

$$t_m \propto \frac{L^2}{D_{\text{eff}}} \quad (4)$$

Table 2 shows the t_m data as a function of temperature, pressure in the column and particle size for industrial polypropylene powders. Although data were made available for both ethylene and propylene, we will only consider those for ethylene for the sake of brevity. The trends and conclusions are identical for both gases studied.

It turns out that this expression provides some very useful information on diffusion in polyolefins powders. It should be briefly pointed out that knowledge of diffusion coefficients or mass transfer times in inert powders is not necessarily equivalent to knowledge of mass transfer rates in polymerising particles (see, e.g. Kittilsen and McKenna [3]). The difficulty of course lies in correctly identifying the characteristic length scale, L , and obtaining experimental data on diffusion coefficients in real particles. If, we can identify L , we can use Eq. (4) to provide information the effective diffusion coefficient for use in model (1), or we can obtain information on L , if we assume that the diffusivity does not vary in particles of a different size (but from the same batch) and look at the influence of changing particle size on t_m .

Let us now reconsider the data for t_m in Table 2. If, we assume (for the moment) that $L \approx r_p$, then it is easy to calculate values for D_{eff} for the different powders used in this study. In most cases, D_{eff} lies between 10^{-6} and $10^{-5} \text{ cm}^2/\text{s}$. If $L \ll r_p$, then the diffusion coefficient would have to be even smaller in order to account for the measured characteristic times. This would not be particularly realistic. So, we can conclude that even if the characteristic length scale for diffusion is not the particle radius, it is not much smaller than r_p . Note that these values of D_{eff} are very close to those measured for diffusion of ethylene (and propylene) in solid polyolefins (e.g. [8]). This means that D_{eff} as pictured in Fig. 2 is essentially equal to the diffusion coefficient of a monomer in solid polymer. This, coupled with the fact that t_m does not vary with pressure [4], but seems to vary only as a function of the particle diameter (at constant temperature) leads us to believe that under the conditions in the column, the major diffusion resistance is in the polymer phase and not in the pores of the macroparticles. We will discuss the implications of this a bit further on in this article.

Closer inspection of the results in also reveals that in some cases (e.g. ATO PP1), t_m scales well as a function

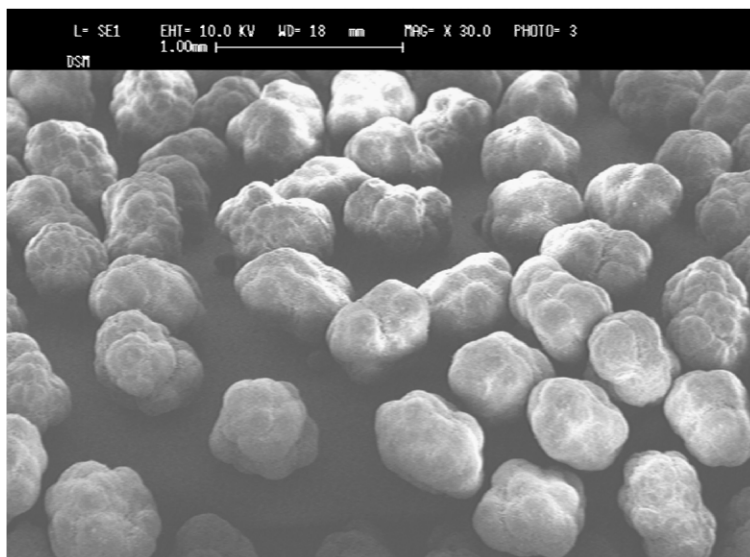


Fig. 3. DSM iPP particles.

of the square of d_p , whereas in others (e.g. DSM isotactic polypropylene (iPP)) it does not. Furthermore, it can be seen from Table 2 that t_m is very different for Solvay PP1, and for Solvay PP2, even though the average particle size used in the experiments is the same.

The reasons for these perhaps unexpected results can be found by examining Figs. 3–6 which show electron micrographs of some of the particles used in this study. The images, while of unique particles, were found to be

representative of a number of particles from each sample, so we can be comfortable drawing conclusions from them. If, we compare the morphologies of Solvay PP1 and of ATO PP1, we can see that these particles exhibit a rather continuous, compact structure, with little apparent macroporosity. However, Solvay PP2 has a very porous, open structure throughout (see Table 1), and DSM iPP seems to be made up of small, bulbous structures that are around one half to one quarter the diameter of the particles themselves. The measurable porosity of DSM iPP was lower than of Solvay PP2, but since the constituent parts of the particles are visible from Fig. 3, the difference between the first group of powders and this one remains clear.

We can therefore, interpret the results of t_m in terms of particle morphology. In the cases where the particles have a closed, compact morphology, the value of t_m scales well with the square of the particle diameter. In these cases, it is reasonable to say that the characteristic length scale for diffusion in the solid portion of the polymer matrix is the radius (or diameter) of the particle. On the other hand, when the value of the characteristic mass transfer time does not scale in this manner, it is clear that the characteristic length scale for diffusion is shorter than the radius of the particle (about one-half to one-fifth). However, even in these cases, the length scale for diffusion remains much larger than the 1 or 2 μm that should be characteristic of diffusion through the microparticles.

A number of remarks need to be made concerning these conclusions. First of all, it is true that examining the electron micrographs in Fig. 3 through Fig. 6 tells us nothing about the microporosity (i.e. pores much smaller than 1 μm in diameter). We can use them to understand the macroscopic morphology of the particles only. The microporosity could theoretically influence the rate of mass transfer, and of course the characteristic length scale for diffusion.

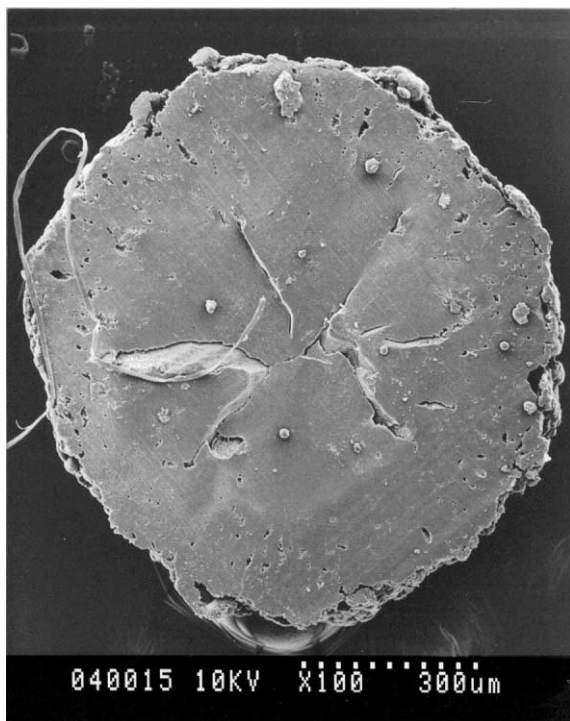


Fig. 4. ATO PP1.

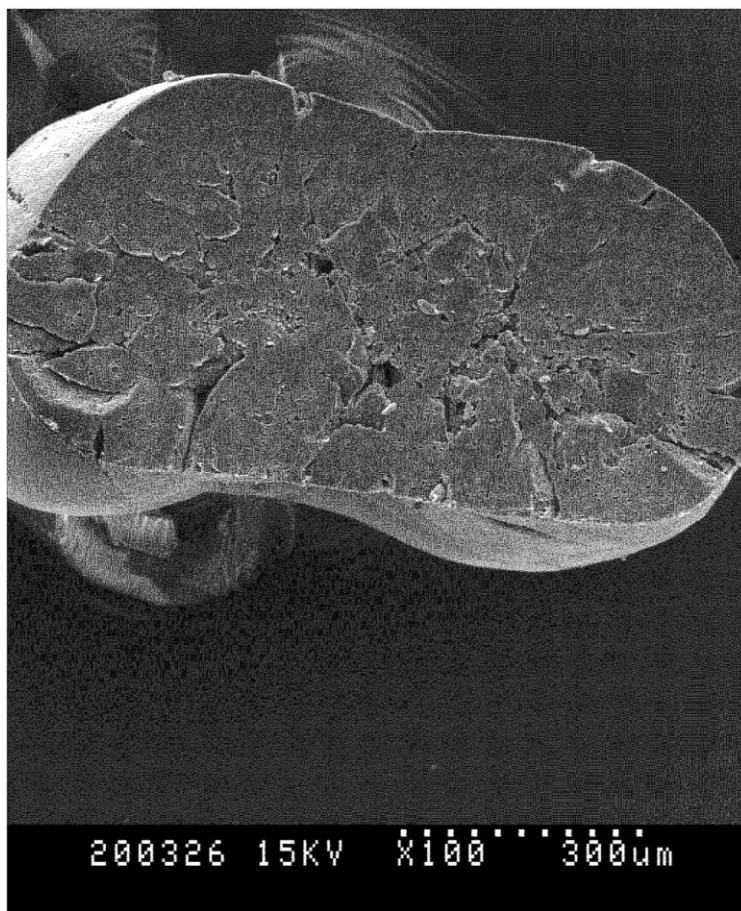


Fig. 5. Morphology of Solvay PP1.

However, if microporosity had a significant impact on mass transfer the effective diffusion coefficients would be higher than what we observe here, and we would see a much weaker dependence of t_m on the particle size. The overall crystallinity of the polymers used herein was very similar (see Table 3), so any differences in the results based on different quantities of amorphous material need to be ruled out. Also, these conclusions implicitly rely on the fact that the effective diffusivity of monomer is the same for different particle cuts coming from the same powder. Examination of particle void fraction by microporosity (not shown here) shows that all of the cuts had the same porosity as the overall powder, which means that this is probably a reasonable assumption.

We can, therefore, re-interpret the data on mass transfer times presented in this work in such a way that it yields at least four major conclusions.

1. The effective diffusion coefficient of gaseous monomers in the particles studied in this work is similar to that in solid polymer.
2. The characteristic mass transfer times in the polymer particles directly correlates with the morphology of the particles.
3. The characteristic length scale for diffusion in some of the industrial polymer particles is equal to, or at least the same order of magnitude as the polymer particles.
4. The value for the effective diffusion coefficient in growing polymer particles is much lower than that typically used in modelling gas phase olefin polymerisation for the particles studied here.

The significance of these results is not negligible, since they do not necessarily coincide with common thinking on the matter of polyolefin particle morphology. First of all,

Table 3
Scaling of d_p^2 with characteristic time

	ATO2/ATO1	SolPP1/ATO1	ATO2/SolPP1	SolPP1/SolPP2
$[d_p(\text{polym1})/d_p(\text{polym2})]_{\text{theor}}^2$	4.6	2.8	1.6	1
$[t_m(\text{polym1})/t_m(\text{polym2})]_{\text{exp}}$	4.3	2.7	1.6	4.8

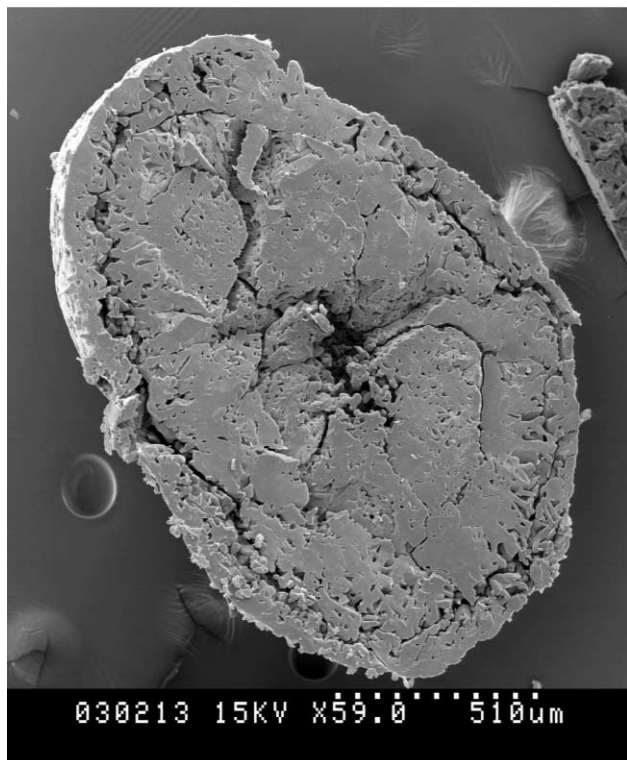


Fig. 6. Morphology of Solvay PP2.

most authors (e.g. [1,2,9–11] just to cite a few) have generally assumed that the effective diffusion coefficient in the macroparticles was equal to that of the monomer in question in the bulk phase (D_{bulk}) multiplied by a correction factor that corresponds to the porosity of the particle (ϵ) divided by a reasonable value of the tortuosity of the pores in the particles (τ)

$$D_{\text{eff}} = D_{\text{bulk}} \frac{\epsilon}{\tau} \quad (5)$$

This approximation led to the use of effective diffusion coefficients two to three orders of magnitude greater than those measured here. Secondly, given that the major resistance to mass transfer seems to be in the polymer phase of the particles, it is also clear that the characteristic length scale for diffusion is certainly much larger than the “microparticles” used in the models mentioned above. If this were not the case, i.e. the characteristic length scale for diffusion in the particles was equivalent to the dimension of the microparticles, then t_m should be much shorter than it has been measured to be, and it should also be entirely independent of the overall particle diameter—which obviously it is not here.

This suggests that the basis for the MGM/PFM models in certain cases needs to be reviewed. Given the structure of a large number of catalyst particles, it is unreasonable to say that the MGM/PFM representation of particle morphology does not repose on a solid, fundamental footing. Electron micrographs of catalyst particles and of particles with relatively little polymer formed on their surface support this

concept (e.g. [12]). However, it is difficult to deny the fact that the morphology of the particles (at least those studied here) seems to evolve as a function of advancement of the reaction.

3.2. Coupled heat and mass transfer

As discussed in [1,2], heat transfer resistance is going to be more important in gas phase polymerisation than in slurry systems. And, although one would suspect that mass transfer is not a problem in the gas phase due to the high diffusivity of the monomer in the pores of the macroparticle, this is not always going to be the case. As discussed above, an evolution of the characteristic length scale of diffusion in the polymer can change this. Since the polymerisation takes place at 80 °C and since it is entirely possible to have large temperature gradients of 20–30 °C between the particle and either the surrounding fluid and/or a neighbouring body in the reactor [1,2,13], it can happen that the particles in a gas phase reactor either melt (e.g. when two hot particles touch each other), or at least reach the softening point which is generally well below the melting point. In either case, this can cause the particles to stick together. Increasing the volume of the particles in this manner will simply compound the overheating problem, and can serve as a “germ” for the formation of agglomerates, or eventually the thermal runaway of the reaction. The consequences of occasional melting and agglomeration can be seen in Figs. 7–9.

Two similar runs for the production of linear low density polyethylene (LLDPE) were carried out on the catalyst VM. In the first of these runs, the monomer feed contained 2.6 mol% butene in order to help accelerate the reaction (it is well known that adding small amounts of higher α -olefins during the polymerisation of ethylene helps to significantly increase the rate of reaction). We can see from Fig. 7a that the average rate of reaction (in the absence of agglomeration or other difficulties) is approximately 16,000 g/g/h (grams of polymer per gram of catalyst per hour). Although not shown here, under exactly the same conditions, the rate of polymerisation during a homopolymerisation (no butene) never exceeded 10,000 g/g/h. In the second run, the activity and productivity of which are shown in Fig. 7b, the butene content of the feed was 3.3%. This slight difference in butene content should not have a significant impact on the rate of reaction (if it did, one would expect the average activity in (b) to be slightly higher). However, we can clearly see that the run in Fig. 7b has a much lower overall activity (average rate of 8200 g/g/h for run b over 30 min versus 16,300 for run a over the same time period), although the initial rate of polymerisation is very similar to that of run (a). In theory, there is no difference between these two runs. However, in run (b) there was a significant amount of agglomeration during the initial stages of reaction. In this case, 28% of the final polymer phase was present in the form of individual lumps, or sheets on the reactor wall and agitator—the rest is in the form of the free flowing powder that we expect

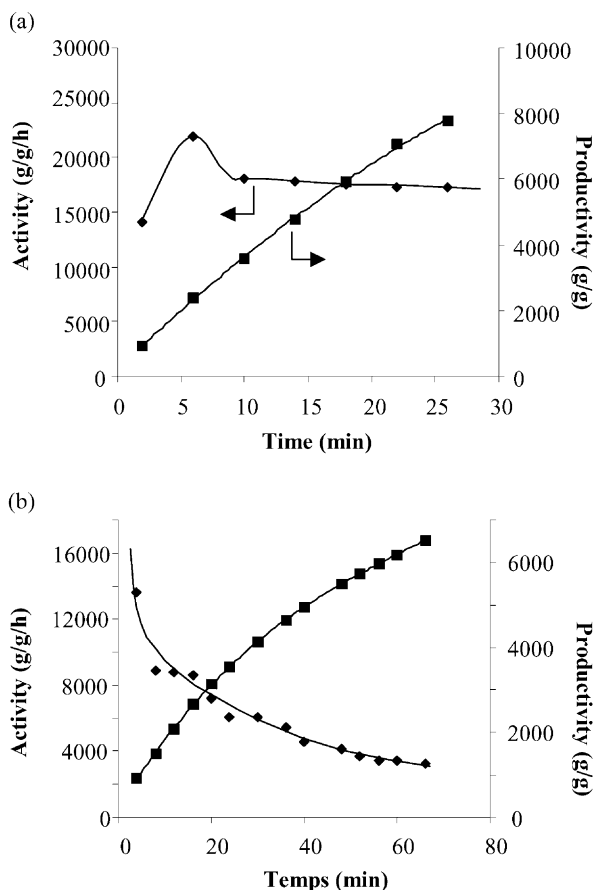


Fig. 7. The activity (g/g/h: grams polymer per gram catalyst per hour) and productivity (g/g: grams polymer per gram catalyst) for two similar runs on catalyst VM. Top figure contained 2.6% butene in the monomer ballast, and bottom run 3.3%. In principle, these differences should not significantly alter the rate of polymerisation. No agglomeration occurred during the run in (a). At the end of the run in (b), 28% of the total mass of polymer formed was in the form of large lumps and strings.

to find. It should be noted that in runs where agglomerates were formed, the reactor vibrated significantly after about 3 to 5 min of polymerisation and the agitator made much more noise than in the case of a run that proceeded without incident. Since, it is not possible to withdraw samples from our semi-batch reactor, it is difficult to tell exactly when the melt-down and agglomeration occurred. Nevertheless, it is likely that this undesirable effect is directly correlated with the unexpected vibrations of the reactor, i.e. that occurs very early during the reaction. Figs. 8 and 9 show that similar results and similar consequences are observed for catalysts T1 and T2 respectively. In both of these cases, the observed reaction rates are very similar in the early stages of reaction, but drop rapidly in cases where agglomeration is observed. In all of these runs, vibration of the lab scale reactor corresponded to formation of lumps. And, as clearly shown in Fig. 9, the more agglomerates are formed, the more severe the effect on the observed rate of polymerisation.

Formation of lumps and agglomerates in the reactor seems to occur with all of the catalysts used here—but only from

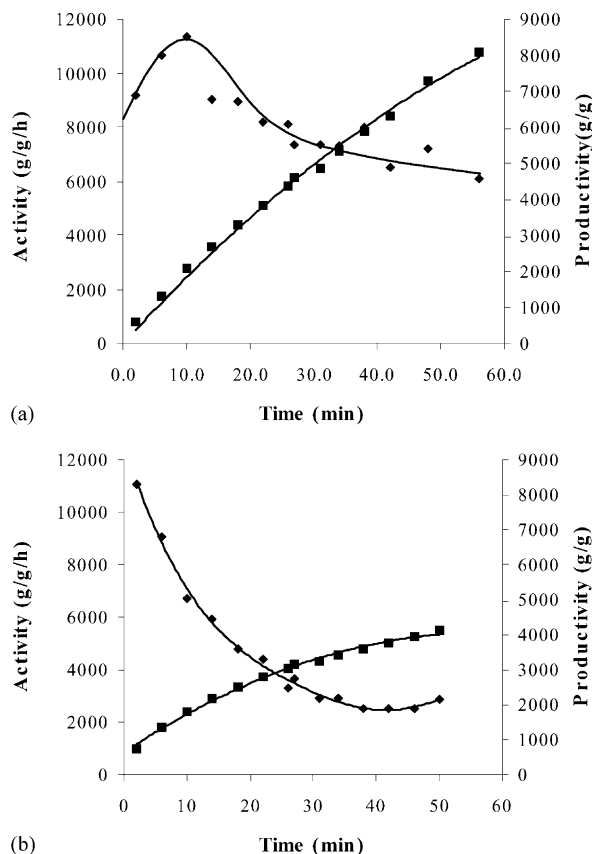


Fig. 8. Production of LLDPE on T1. No agglomerates were found for the run presented in (a). All conditions identical, except for the formation of agglomerates equal to 10% of the final mass of polymer in (b).

time-to-time (only 25–30% of all gas phase reactions lead to significant formation of agglomerates). It is a reproducible phenomenon in the sense that its impact on the reaction rate is always the same, but (fortunately) does not occur during all polymerisation reactions in the gas phase. Many modelling studies (e.g. [1,2,9,10,12,13]) have shown that if heat transfer limitations (i.e. overheating of the growing particles)

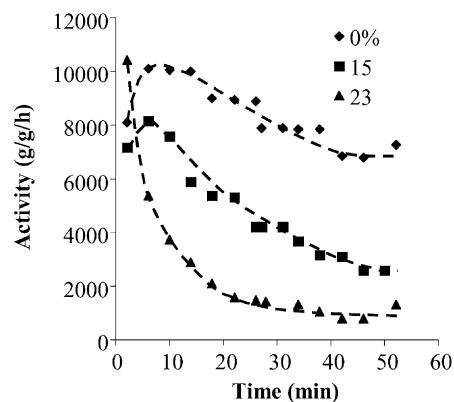


Fig. 9. Activities of three different runs on catalyst T2. All runs should be similar, but had different amounts of agglomerates (see key) at the end of the reaction.

are to be observed, this will happen during the first few minutes of the polymerisation reaction. In addition, McKenna et al. [13] showed that significant amounts of heat transfer can occur through particle–particle interaction during gas phase polymerisation. In this last work, it was shown that large particles (even if they are still polymerising) can act as heat sinks for the smaller particles that are in contact with them. On the other hand, if two small particles come into contact, the risk of overheating and meltdown is much higher. It is common practice (at least on the laboratory scale) to use either an inert powder (as we do), or another product such as rock salt as an initial charge in the reactor to help disperse the catalyst particles and to help avoid having them come into contact during the early stages of the reaction. It is possible that in our experimental procedure that we do not use enough inert powder. This means that small, hot particles might come into contact more often than is desirable, thus leading to occasional meltdown and formation of agglomerates. This could certainly explain the seemingly random character of the phenomena observed over the course of a number of reactions.

Nevertheless, this formation of lumps and agglomerates has a significant impact on the mass transfer rates in the reactor, and thus on the material properties of the final products. As we mentioned above, one would not expect significant problems related to mass transfer in gas phase reactions since the diffusivity of the monomers is relatively high, and the length scale for mass transfer through the polymer layer surrounding the active sites is so low. However, a change in the length scale for diffusion through the polymer could change this. In effect, this is what happens when the polymer particles melt and agglomerate to form lumps of several millimetres or even centimetres in diameter. In this case, the length scale for diffusion of monomer through the polymer changes by two to three orders of magnitude, thus changing the characteristic time for mass transfer by four to six orders of magnitude. Clearly, diffusion through the polymer is the rate limiting step in the agglomerated phase. This causes the reaction rate to slow down as significantly less monomer is reaching the active sites—only those active sites not trapped in the agglomerated phase will polymerise “normally”. In addition, since the average molecular weight of the polymer is proportional to the monomer concentration at the active sites [14], one would expect to find very different polymer in the lumps and sheets than in the gas phase.

To separate the free and the agglomerated particles of the polymer, we sieved the powder, which allowed us to measure the molecular weight of the two “different” phases. The molecular weight of each fraction was measured by measuring the melt flow index. If we compare the results of the measurement of the molecular weight of the free flowing powder with that of the agglomerated parts of the reaction mass, we can see that there is indeed a noticeable difference (Table 4). The molecular weight of the agglomerated material is approximately 25% lower than that of the free flowing powder. This means that the concentration of monomer in the

Table 4
Molecular weights for free flowing and agglomerated powders^a

Catalyst	Agglomeration (mass % w.r.t. final product)	Free flowing powder		Agglomerates	
		M_w	I	M_w	I
T1	0	144	8.7	–	–
T1	12	154	8.8	128	8.6
T1	18	143	8.7	131	9.1
T2	0	147	8.5	–	–
T2	15	131	8.4	102	8.6
T2	16	130	8.3	130	8.3
T2	21	136	8.4	136	8.4
T2	23	113	8.5	97	8.7

^a M_w , weight average molecular weight; I , polydispersity index.

agglomerated portion of the reaction mass was clearly lower than that in the rest of the powder, and that we experienced mass transfer resistance in the same portion of the powder as where we also encountered heat transfer problems.

4. Conclusions

If, we limit our conclusions only to the particles studied here, it is possible that the scheme presented in Fig. 10 explains how the morphology of the particles evolves. In this proposed scheme, the catalyst and prepolymer particles (i.e. particles with “low” degree of polymerisation) retain an MGM-type morphology where the particle is an assembly of micrograins that expand during the early stages of polymerisation. As the reaction advances, neighbouring micrograins “meld” into larger agglomerates. Whereas the MGM considers that a micrograin contains one (or at most a small number of) catalyst fragments, these agglomerates would contain several fragments. The existence of such structures has been proposed by Kittilsen and McKenna

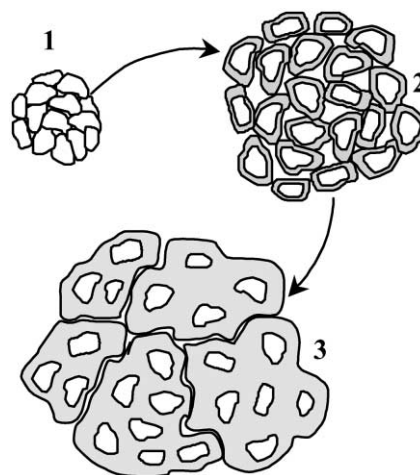


Fig. 10. Scheme of proposed particle growth model, where catalyst (1), and prepolymer particle (2) retain “MGM-style” morphology, and polymer particle (3) assumes a more or less agglomerated structure as the reaction proceeds.

[15] for the specific case of impact polypropylene, but the evidence presented in the current paper suggests that such structures can occur in a wide number of polyolefins systems. The determination of the rate at which this agglomeration of micrograins would occur (if indeed it does happen), the transition from MGM-type morphology to more complex structures will require a significant amount of work. The exact evolution will of course depend on a number of factors including temperature, polymer composition, phases present in the reactor, rate of production of polymer, and the type of support. It is important to mention that all of the catalyst systems used to prepare the polymers used in the columns, and in [12,15] were prepared on MgCl_2 supports, so one should not generalise the results reported herein for other systems (e.g. silica, or chromium systems).

However, in the systems where an evolution of the morphology occurs, it will certainly pose a difficult problem for the modelling of heat and mass transfer given that the effective diffusivity will drop by up to three orders of magnitude from a value of around $10^{-4} \text{ cm}^2/\text{s}$ at the beginning of the reaction. As this occurs, there will be a change in the length scale of diffusion in the growing particles. The combined increase in length scale and decrease in effective diffusivity might create certain difficulties at the level of mass transfer within the particles. While there is little to no evidence supporting the presence of mass transfer resistance during gas phase polymerisation (e.g. [1,2,11]), most of the work done in this area has been on homopolymerisation (or on the production of linear low density polyethylene, which is a co-polymer of ethylene with a small amount of butene). However, it is shown in [3] that reductions in the effective diffusivity in a growing particle can lead to accumulation of species such as propylene during the production of EPR. It is, therefore, important to pursue this issue in more detail in further work.

While it is not entirely clear why heat transfer problems occur seemingly randomly in 25–30% of the gas phase reactions run on the three catalyst systems used here, it is clear that the changes of length scale associated with partial melting and agglomeration of the particles have an impact on mass transfer during the polymerisation. The rate of reaction is a function of the amount of agglomerate formation in the reaction, and will drop significantly as more agglomerates are formed since this increases the length scale for diffusion, and thus leads to a drop in the diffusive flux of monomer to the active sites. Since it is impossible to really know how many of the catalyst particles are trapped inside large lumps or sheets of polymer it is difficult to correlate the observed decrease in the rate of reaction with the amount of agglomerates formed. Nevertheless, the drop in the reaction rate coupled with the differences observed in the molecular weights between the agglomerated and non-agglomerated particles establishes a link between heat and mass transfer in these polymerising systems.

Full models for particle growth must, therefore, include the impact of morphological changes that can occur during the polymerisation reaction. A more accurate description of heat transfer is needed (e.g. [12]), and temperature and concentration profiles need to be better associated with the material properties of the polymers in question if we want to develop full, quantitative models that allow us to associate local conditions in the reactor with final polymer properties.

Acknowledgements

The authors wish to acknowledge the financial support of the European Commission (contract BE96-3022 CATAPOL), and gratefully acknowledge the permission of Solvay, DSM and ATOFINA to publish the images of the polymer particles in this work. SEM images were made at the Centre de Microscopie Electronique of the Université Claude Bernard Lyon I. The authors also wish to thank Jean-Pierre Broyer of the LCPP for his help with the experimental aspects of the polymerisation reaction and polymer characterisation.

References

- [1] S. Floyd, K.Y. Choi, T.W. Taylor, W.H. Ray, Polymerization of olefins through heterogeneous catalysis. Part III. Polymer particle modelling with an analysis of intraparticle heat and mass transfer effects, *J. Appl. Polym. Sci.* 32 (1986) 2935–2960.
- [2] S. Floyd, K.Y. Choi, T.W. Taylor, W.H. Ray, Polymerization of olefins through heterogeneous catalysis. Part IV. Modeling of heat and mass transfer resistance in the polymer particle boundary layer, *J. Appl. Polym. Sci.* 31 (1986) 2231–2265.
- [3] P. Kittilsen, T.F. McKenna, Modelling of Transfer Phenomena on Heterogeneous Ziegler Catalysts: Part 4. Convection effects in gas phase processes, *Chem. Eng. Sci.* 56 (13) (2001) 3997–4005.
- [4] A. Sliepcevich, G. Storti, M. Morbidelli, Measurement of diffusivity and solubility of olefins in polypropylene by gas chromatography, *J. Appl. Polym. Sci.* 78 (2000) 464–473.
- [5] C. Martin, Ph.D. Thesis, Université Claude Bernard Lyon I, July 2000.
- [6] N. Verdel, Influence du Choix du Procédé sur la sélectivité des Catalyseurs Métalloènes de Polymérisation des Oléfines Ph.D. Thesis, University Claude Bernard Lyon-I, No 302.97, 1997.
- [7] V. Mattioli, Transferts de Matière et de Chaleur en Polymérisation des Oléfines sur Catalyseur Ziegler–Natta, Ph.D. Thesis, University Claude Bernard Lyon-I, No 055-2000, 2000.
- [8] A.S. Michaels, H.J. Bixler, Flow of gases through polyethylene, *J. Polym. Sci. L* 50 (1961) 413–439.
- [9] R.A. Hutchinson, C.M. Chen, W.H. Ray, Polymerization of olefins through heterogeneous catalysis. Part X. Modeling of particle growth and morphology, *J. Appl. Polym. Sci.* 44 (1992) 1389–1414.
- [10] R.L. Laurence, M.G. Chiovetta, Heat and mass transfer during olefin polymerization from the gas phase, in: K.H. Reichert, W. Geisler (Eds.), *Polymer Reaction Engineering: Influence of Reaction Engineering on Polymer Properties*, Hanser Publishers, Munich, 1983.
- [11] T.F. McKenna, J. DuPuy, R. Spitz, Modelling of transfer phenomena on heterogeneous ziegler catalysts: differences between theory and

- experiment, an introduction, *J. Appl. Polym. Sci.* 57 (1995) 371–384.
- [12] T.F. McKenna, D. Cokljat, R. Spitz, D. Schweich, Modelling of heat and mass transfer during the polymerisation of olefins on heterogeneous ziegler catalysts, *Catal. Today* 48 (1–4) (1999) 101–108.
- [13] T.F. McKenna, D. Cokljat, R. Spitz, Heat transfer from heterogeneous catalysts: an exploration of underlying mechanisms using CFD, *AIChE J.* 45 (11) (1999) 2392–2410.
- [14] T.F. McKenna, F. Barbotin, R. Spitz, Modelling of transfer phenomena on heterogeneous Ziegler catalysts. Part 2. Experimental investigation of intraparticle mass transfer resistance during the polymerisation of ethylene in slurry, *J. Appl. Polym. Sci.* 62 (1997) 1835–1841.
- [15] P. Kittilsen, T.F. McKenna, A study of the kinetics, mass transfer and particle morphology in the production of high impact polypropylene, *J. Appl. Polym. Sci.*, submitted for publication.